Supernova Inelastic Neutrino-Nucleus Cross Sections from High-Resolution Electron Scattering Experiments and Shell-Model Calculations

K. Langanke,[1] G. Martínez-Pinedo,[2] P. von Neumann-Cosel,[3] and A. Richter[3]

[1]*Institute for Physics and Astronomy, University of Århus, DK-8000 Århus C, Denmark*
[2]*ICREA and Institut d'Estudis Espacials de Catalunya, Edifici Nexus, Gran Capità 2, E-08034 Barcelona, Spain*
[3]*Institut für Kernphysik, Technische Universität Darmstadt, 64289 Darmstadt, Germany*

(Received 2 February 2004; published 11 November 2004)

Highly precise data on the magnetic dipole strength distributions from the Darmstadt electron linear accelerator for the nuclei ^{50}Ti, ^{52}Cr, and ^{54}Fe are dominated by isovector Gamow-Teller-like contributions and can therefore be translated into inelastic total and differential neutral-current neutrino-nucleus cross sections at supernova neutrino energies. The results agree well with large-scale shell-model calculations, validating this model.

DOI: 10.1103/PhysRevLett.93.202501 PACS numbers: 21.60.Cs, 25.30.Dh, 25.30.Pt, 27.40.+z

Knowledge about inelastic neutrino-nucleus scattering plays an important role in many astrophysical applications, including r-process nucleosynthesis, the synthesis of certain elements such as ^{10,11}B and ^{19}F during a supernova explosion by the ν process or for the detection of supernova neutrinos (e.g., see [1]). Although inelastic neutrino-nucleus scattering is not yet considered in supernova simulations, model studies have indicated that it might be relevant to several aspects of supernova physics (i) for the neutrino opacities and thermalization during the collapse phase [2], (ii) for the revival of the stalled shock in the delayed explosion mechanism [3,4], and (iii) for explosive nucleosynthesis [5]. To predict the outcome of supernova simulations with confidence, a better handle on neutrino-nucleus interactions is called for [4], in particular, on nuclei in the iron mass range $A \sim 56$ [5]. While charged-current neutrino-nucleus reactions—the inverse of electron and positron captures—are included in supernova simulations [6], inelastic neutrino-nucleus scattering is not. Unfortunately, no data for inelastic neutrino-nucleus scattering are currently available (except for the ground state transition to the $T = 1$ state at 15.11 MeV excitation energy in ^{12}C [7,8]). To measure some relevant neutrino-nucleus cross sections (mainly in the iron mass range), a dedicated detector at the Oak Ridge spallation neutron source has been proposed [1]. To sharpen the experimental program at this facility and to improve supernova simulations, inelastic neutrino-nucleus cross sections should be incorporated into the supernova models. It appears as if the needed inelastic neutrino cross sections for iron-region nuclei have to be evaluated by theoretical models without constraint by data. This Letter will demonstrate that this is in fact not the case. Our aim is to show that precision data on the magnetic dipole ($M1$) strength distributions, obtained by inelastic electron scattering, supply to a large extent the required information about the nuclear Gamow-Teller (GT) distribution which determines the inelastic neutrino-nucleus cross sections for supernova neutrino energies. This intimate relation of $M1$ and GT strengths has already been exploited before to estimate neutrino cross sections for either individual transitions (e.g., in ^{12}C [9,10]) or total cross sections (e.g., in ^{208}Pb [11,12]). We will add to this by demonstrating that large-scale shell-model calculations agree quite well with the precision $M1$ data, thus validating the use of such models to determine the required cross sections for nuclei where no data exist, or at the finite-temperature conditions in a supernova.

The $M1$ response is one of the fundamental low-energy excitations of the nucleus. It can be well explored by means of inelastic electron scattering. Such transitions are mediated by the operator

$$\boldsymbol{O}(M1) = \sqrt{\frac{3}{4\pi}}\sum_k [g_l(k)\boldsymbol{l}(k) + g_s(k)\boldsymbol{s}(k)]\mu_N, \qquad (1)$$

where $\boldsymbol{l}$ and $\boldsymbol{s}$ are the orbital and spin angular momentum operators, and the sum runs over all nucleons. The orbital and spin gyromagnetic factors are given by $g_l = 1$ and $g_s = 5.586$ for protons, and $g_l = 0$ and $g_s = -3.826$ for neutrons [13]; μ_N is the nuclear magneton. Using isospin quantum numbers $\pm 1/2$ for protons and neutrons, respectively, and $\boldsymbol{t}_0 = \boldsymbol{\tau}_0/2$, Eq. (1) can be rewritten in isovector and isoscalar parts. Because of a strong cancellation of the g factors in the isoscalar part, the isovector part dominates. The respective isovector $M1$ operator is given by

$$\boldsymbol{O}(M1)_{\rm iv} = \sqrt{\frac{3}{4\pi}}\sum_k [\boldsymbol{l}(k)\boldsymbol{t}_0(k) + (g_s^p - g_s^n)\boldsymbol{s}(k)\boldsymbol{t}_0(k)]\mu_N. \qquad (2)$$

We note that the spin part of the isovector $M1$ operator is the zero component of the GT operator,

$$\boldsymbol{O}(\mathrm{GT}_0) = \sum_k \boldsymbol{\sigma}(k)\boldsymbol{t}_0(k) = \sum_k 2\boldsymbol{s}(k)\boldsymbol{t}_0(k), \qquad (3)$$

however, enhanced by the factor $\sqrt{3/4\pi}(g_s^p - g_s^n)\mu_N/2 = 2.2993\mu_N$. On the other hand, inelastic neutrino-nucleus scattering at low energies, where finite-momentum transfer corrections can be neglected, is dominated by allowed transitions. The cross section for a transition from an initial nuclear state (i) to a final state (f) is given by [10]

$$\sigma_{i,f}(E_\nu) = \frac{G_F^2 g_A^2}{\pi(2J_i+1)}(E_\nu - \omega)^2 |\langle f || \sum_k \sigma(k) \boldsymbol{t}(k) || i \rangle|^2, \tag{4}$$

where G_F and g_A are the Fermi and axial vector coupling constants, respectively, E_ν is the energy of the scattered neutrino, and ω is the difference between final and initial nuclear energies. Note that for ground state transitions $E_x = \omega$. The nuclear dependence is contained in the $B(\mathrm{GT}_0) = g_A^2 |\langle f || \sum_k \sigma(k) \boldsymbol{t}(k) || i \rangle|^2/(2J_i+1)$ reduced transition probability between the initial and final nuclear states.

Thus, experimental $M1$ data yield the desired GT_0 information, required to determine inelastic neutrino scattering on nuclei at supernova energies, to the extent that the isoscalar and orbital pieces present in the $M1$ operator can be neglected. On general grounds, one expects that the isovector component dominates over the isoscalar piece. Furthermore, it is well known that the major strength of the orbital and spin $M1$ responses are energetically well separated in the nucleus. In pf-shell nuclei, which are of interest for supernova neutrino-nucleus scattering, the orbital strength is located at excitation energies $E_x \simeq 2$–4 MeV [14], while the spin $M1$ strength is concentrated between 7 and 11 MeV. A separation of spin and orbital pieces is further facilitated by the fact that the orbital part is strongly related to nuclear deformation [15]. For example, the scissors mode [16], which is the collective orbital $M1$ excitation, has been detected in well-deformed nuclei such as ^{56}Fe [17]. Thus one can expect that in spherical nuclei the orbital $M1$ response is not only energetically well separated from the spin part but also strongly suppressed.

Examples of spherical pf-shell nuclei are ^{50}Ti, ^{52}Cr, and ^{54}Fe. As these nuclei have also the advantage that precise $M1$ response data exist from high-resolution inelastic electron scattering experiments [18], we have chosen these three nuclei for our further investigation. Our strategy now is to show, in a detailed comparison of data and shell-model calculations, that the $M1$ data indeed represent the desired GT_0 information in a sufficient approximation to transform them into total and differential neutrino-nucleus cross sections. All the total strengths and the strength functions of ^{50}Ti have been computed using the code NATHAN [19], and the KB3G residual interaction [20] in the complete pf model space (orbits $f_{7/2}$, $p_{3/2}$, $p_{1/2}$, and $f_{5/2}$). For ^{52}Cr and ^{54}Fe the strength functions are computed in truncated model spaces, allowing up to six and five protons and neutrons to be promoted from the lowest $f_{7/2}$ orbital into the other pf-shell orbitals, respectively. The $M1$ and GT_0 response functions are calculated with 400 Lanczos iterations for both isospin channels. As is customary in shell-model calculations, the spin operator is replaced by an effective operator $\boldsymbol{s}_{\mathrm{eff}} = 0.75\boldsymbol{s}$, where the constant is universal for all pf-shell nuclei [21].

Experimentally, $M1$ data have been determined for the energy intervals 8.5–11.6 MeV in ^{50}Ti (resolving the $M1$ strength for 29 individual states), while for the other two nuclei $M1$ data exist for the energy interval 7.0–11.8 MeV, resolving 53 states for ^{52}Cr and 33 states for ^{54}Fe. The summed experimental $B(M1)$ strength (in μ_N^2) in these intervals is 4.5(5) for ^{50}Ti, 8.1(5) for ^{52}Cr, and 6.6(4) for ^{54}Fe, which for ^{50}Ti and ^{52}Cr is in agreement with the shell model (4.3 and 7.6, respectively, in the same intervals). For ^{54}Fe the shell-model strength is slightly larger (8.6) than the data, which is also true if the residual interaction GXPF1 [22] is used (8.4). The total shell-model $B(M1)$ strengths of 7.2 for ^{50}Ti, 8.7 for ^{52}Cr, and 10.2 for ^{54}Fe indicate some additional strength outside of the experimental energy window. For a comparison of the $M1$ strength distributions a problem arises due to uncertainties of the distinction between $M1$ and $M2$ transitions in some of the (e, e') data. Therefore, all possible $M1$ candidates are modified by the weighing factors introduced in [18] to express the level of confidence of the assignment. The experimental sensitivity limit $B(M1) \simeq 0.04\mu_N^2$ is also taken into account for comparison with the model results. It should be noted that, where data are available [23,24], good agreement with nuclear resonance fluorescence experiments is observed for the prominent $M1$ transitions. This is also the case for other pf-shell nuclei [25,26]. For all nuclei, the energy dependence of the observed $M1$ strength distribution is well reproduced. This is shown in Fig. 1 for the example of ^{52}Cr.

To determine how well the $M1$ data might reflect the desired GT_0 information, we have performed shell-model calculations for the individual orbital and spin parts of the $M1$ operator as well as calculations for the GT_0 operator, which, except for a constant factor, represents the isovector spin contribution to the $M1$ operator. The results are displayed in Fig. 1. As expected for spherical nuclei, the orbital $M1$ strength is significantly smaller, by about an order of magnitude, than the spin $M1$ strength. The interference between the orbital and spin parts is state dependent and is largely canceled out, when the strength is averaged over several states. A similar situation occurs for the isoscalar spin contribution, but now its contribution to the total strength is even smaller.

Supernova simulations require differential neutrino-nucleus cross sections as functions of initial and final neutrino energies, where neutrinos of different flavors are comprised in energy bins of a few MeV [27–29]; i.e., cross sections are averaged over many final nuclear states. Canceling most of the interference between orbital and spin contributions, the $M1$ data should represent the

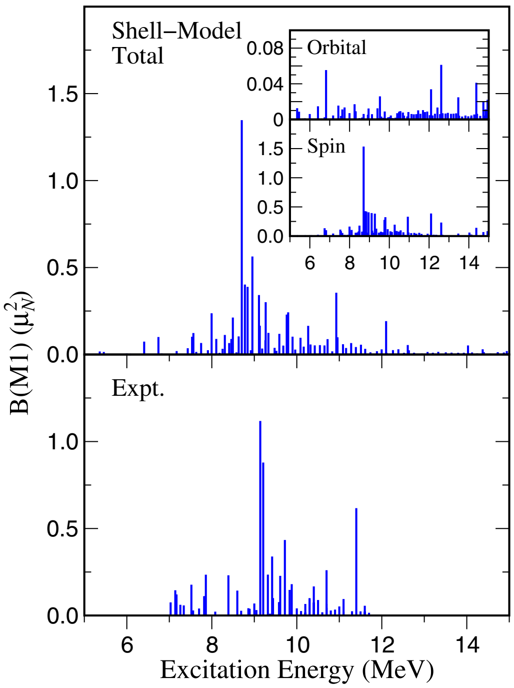

FIG. 1 (color online). Comparison of experimental $M1$ strength distribution $[B(M1) = |\langle f||\boldsymbol{O}(M1)||i\rangle|^2/(2J_i + 1)]$ in ^{52}Cr (bottom) with the shell-model result (top). The inset shows the decomposition into spin (botton) and orbital (top) parts. Note the different scales of the ordinate for the spin and orbital pieces, respectively.

desired GT_0 information, simply using the relation $B(M1) = 3(g_s^p - g_s^n)^2\mu_N^2/(16g_A^2\pi)B(\mathrm{GT}_0)$. Figure 2 compares the total neutrino-nucleus cross sections for the three nuclei, calculated from the experimental $M1$ data with those obtained from the shell-model GT_0 distribution. As some of the $M1$ strength is predicted to reside outside of the currently explored experimental energy window, we have corrected for this by multiplying the "$M1$ cross section" with the ratio $B(\mathrm{GT}_0)/B(\mathrm{GT}_0, \Delta E)$, where ΔE defines the experimental energy interval and the ratio is taken from the shell-model calculations. Based on the above theoretical discussion, one can assume that the (energetically complete) $M1$ cross section represents the neutrino-nucleus cross sections quite well.

Figure 3 shows the differential neutrino cross section for ^{52}Cr at two representative supernova neutrino energies. The cross sections, obtained from the experimental $M1$ data and the shell model, agree quite well, if binned in energy intervals of a resolution (1 MeV or somewhat larger) as required in supernova simulations.

The comparison of $M1$ and theoretical cross sections suggests that shell-model based calculations of inelastic neutrino scattering at supernova-relevant energies are quite accurate and hence the shell model is the method of choice to determine the cross section for the many nuclei in the iron mass region needed in core-collapse simulations. However, such cross sections require additional considerations so far neglected. These must include the effects of finite-momentum transfer, of the finite-temperature in the supernova environment, and the contributions of additional (forbidden) multipoles to the cross section. The latter becomes relevant only for neutrino energies which are sufficiently larger than the centroid energy of the respective giant resonance of this multipole. At such neutrino energies the cross section depends only on the total strength of the multipole and its approximate centroid energy (and not on a detailed reproduction of the strength distribution) and is well described within the random phase approximation (RPA) [30]. We have calculated the RPA contribution to the cross section arising from multipoles other than GT_0, using the formalism of [30,31] which explicitly considers the finite-momentum dependence of the multipole operators. For the GT_0 component the finite-momentum transfer, corrections can be considered as described in [32]. Following the approach of [33] we have derived the finite-temperature corrections

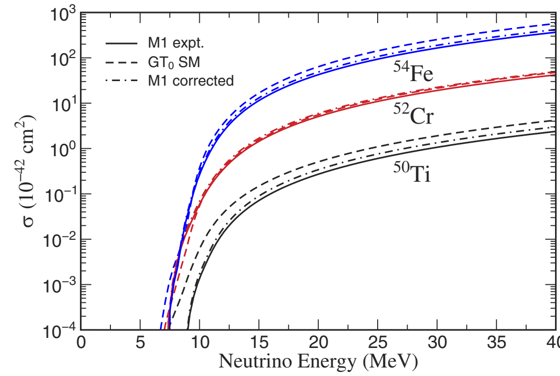

FIG. 2 (color online). Neutrino-nucleus cross sections, calculated from the $M1$ data (solid lines) and the shell-model (SM) GT_0 distributions (dashed lines) for ^{50}Ti (multiplied by 0.1), ^{52}Cr, and ^{54}Fe (times 10). The dash-dotted lines show the cross sections from the $M1$ data, corrected for possible strength outside the experimental energy window.

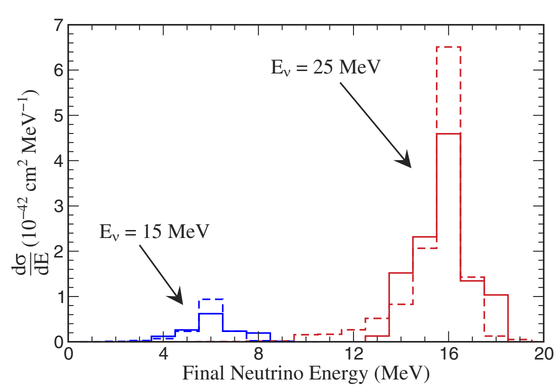

FIG. 3 (color online). Differential inelastic neutrino cross sections for ^{52}Cr and initial neutrino energies $E_\nu = 15$ and 25 MeV. The solid histograms are obtained from the $M1$ data, the dashed histogram from shell-model calculations. The final neutrino energies are given by $E_f = E_\nu - \omega$.

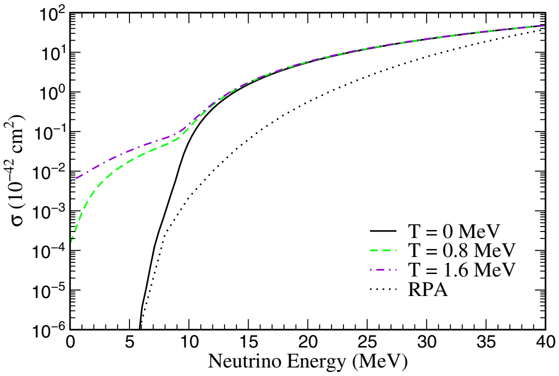

FIG. 4 (color online). Inelastic neutrino scattering cross section on ^{52}Cr, calculated on the basis of shell-model GT$_0$ distributions at finite temperatures. The dotted curve represents the RPA contributions of other multipoles to the cross sections, including finite-momentum transfer corrections.

to the cross sections from the shell-model GT$_0$ transitions between a few hundred excited states and the six lowest nuclear states. The ^{52}Cr cross sections are presented in Fig. 4. Because of the thermal population of excited initial states, the neutrino cross sections are significantly enhanced at low energies during the early collapse phase ($E_\nu \sim 10$ MeV). Once the neutrino energy is large enough to allow scattering to the centroid of the GT$_0$ strength, which resides at energies around 8–11 MeV, finite-temperature effects become unimportant and the neutrino cross section can be derived effectively from the ground state distribution, as discussed in [33], and thus is directly constrained by the $M1$ data. This applies to the neutrino energy regime relevant to postshock supernova simulations. Contributions from multipoles other than the GT$_0$ become important for $E_\nu > 20$ MeV and dominate for energies higher than 35 MeV.

In summary, we have translated the highly precise (e, e') $M1$ data for ^{50}Ti, ^{52}Cr, and ^{54}Fe into detailed total and differential inelastic neutral-current neutrino-nucleus cross sections. Besides representing for the first time detailed neutral-current cross sections for nuclei, such data are, in particular, important for supernova simulations as they allow one to constrain theoretical models needed to derive the inelastic neutrino-induced cross sections for the many nuclei in the medium-mass range present in a supernova environment. We have further demonstrated that large-scale shell-model calculations are able to describe the data, even in details. Following this validation, shell-model calculations for inelastic neutrino cross sections on supernova-relevant nuclei are now in progress.

K. L. is partly supported by the Danish Research Council. G. M. P. is supported by the Spanish MCyT and by the European Union ERDF under Contracts No. AYA2002-04094-C03-02 and No. AYA2003-06128. P. v. N. C. and A. R. acknowledge support by the DFG under Contract No. SFB 634. Computational cycles were provided by the Centre for Scientific Computing in Århus.

[1] Special issue on Neutrino Physics at Spallation Neutron Sources, edited by F. T. Avignone, L. Chatterjee, Y. V. Efremenko, and M. Strayer [J. Phys. G **29**, 2497 (2003)].
[2] S. W. Bruenn and W. C. Haxton, Astrophys. J. **376**, 678 (1991).
[3] W. C. Haxton, Phys. Rev. Lett. **60**, 1999 (1988).
[4] A. B. Balantekin and G. M. Fuller, J. Phys. G **29**, 2513 (2003).
[5] W. R. Hix, A. Mezzacappa, O. E. B. Messer, and S. W. Bruenn, J. Phys. G **29**, 2523 (2003).
[6] S. W. Bruenn, Astrophys. J. Suppl. Ser. **58**, 771 (1985).
[7] B. Zeitnitz, Prog. Part. Nucl. Phys. **32**, 351 (1994).
[8] L. B. Auerbach *et al.*, Phys. Rev. C **64**, 065501 (2001).
[9] W. C. Haxton, Phys. Lett. B **76**, 165 (1978).
[10] T. W. Donnelly and R. P. Peccei, Phys. Rep. **50**, 1 (1979).
[11] G. M. Fuller, W. C. Haxton, and G. C. McLaughlin, Phys. Rev. D **59**, 085005 (1999).
[12] N. Jachowicz, K. Heyde, and J. Ryckebusch, Phys. Rev. C **66**, 055501 (2002).
[13] P. J. Mohr and B. N. Taylor, Rev. Mod. Phys. **72**, 351 (2000).
[14] T. Guhr *et al.*, Z. Phys. A **336**, 159 (1990).
[15] J. Enders, H. Kaiser, P. von Neumann-Cosel, C. Rangacharyulu, and A. Richter, Phys. Rev. C **59**, R1851 (1999).
[16] D. Bohle *et al.*, Phys. Lett. B **137**, 27 (1984).
[17] R. W. Fearick *et al.*, Nucl. Phys. **A727**, 41 (2003).
[18] D. I. Sober *et al.*, Phys. Rev. C **31**, 2054 (1985).
[19] E. Caurier *et al.*, Phys. Rev. C **59**, 2033 (1999).
[20] A. Poves, J. Sánchez-Solano, E. Caurier, and F. Nowacki, Nucl. Phys. **A694**, 157 (2001).
[21] P. von Neumann-Cosel, A. Poves, J. Retamosa, and A. Richter, Phys. Lett. B **443**, 1 (1998).
[22] M. Honma, T. Otsuka, B. A. Brown, and T. Mizusaki, Phys. Rev. C **69**, 034335 (2004).
[23] U. E. P. Berg *et al.*, Phys. Lett. B **103**, 301 (1981).
[24] C. Wesselborg, in *Proceedings of the 8th International Symposium on Capture Gamma Ray Spectroscopy*, edited by J. Kern (World Scientific, Singapore, 1993), p. 89.
[25] A. Degener *et al.*, Nucl. Phys. **A513**, 29 (1990).
[26] F. Bauwens *et al.*, Phys. Rev. C **62**, 024302 (2000).
[27] M. Liebendörfer *et al.*, Astrophys. J. Suppl. Ser. **150**, 263 (2004).
[28] M. Rampp and H.-T. Janka, Astron. Astrophys. **396**, 361 (2002).
[29] A. Burrows, T. Young, P. Pinto, R. Eastman, and T. A. Thompson, Astrophys. J. **539**, 865 (2000).
[30] E. Kolbe, K. Langanke, G. Martínez-Pinedo, and P. Vogel, J. Phys. G **29**, 2569 (2003).
[31] E. Kolbe, K. Langanke, and P. Vogel, Nucl. Phys. **A652**, 91 (1999).
[32] J. Toivanen, E. Kolbe, K. Langanke, G. Martínez-Pinedo, and P. Vogel, Nucl. Phys. **A694**, 395 (2001).
[33] J. M. Sampaio, K. Langanke, G. Martínez-Pinedo, and D. J. Dean, Phys. Lett. B **529**, 19 (2002).